Determination of conduction band offsets in type-II $In_{0.27}Ga_{0.73}Sb/In_xAl_{1-x}As_ySb_{1-y}$ heterostructures grown by molecular beam epitaxy

E. R. Glaser, R. Magno, B. V. Shanabrook, and J. G. Tischler
Naval Research Laboratory, Washington, DC 20375-5347, USA
(Received 5 September 2006; published 5 December 2006)

Low-temperature photoluminescence (PL) has been performed on a set of specially designed $In_{0.27}Ga_{0.73}Sb/In_xAl_{1-x}As_ySb_{1-y}$ multiple quantum well (MQW) heterostructures grown by molecular beam epitaxy in order to provide a measure of the conduction band offsets in this material system. These alloys are of interest for the development of high-speed heterojunction bipolar transistors (HBTs) that show promise for operation at lower power dissipation than in GaAs- and InP-based HBTs. Excitation power studies revealed evidence for strong electron-hole recombination at 0.56 eV within the InGaSb layers of the type-I MQW structure with $(x=0.52, y=0.25)$, while several weaker indirect transitions involving electrons in the $In_xAl_{1-x}As_ySb_{1-y}$ and holes in the InGaSb layers were observed between 0.38 and 0.53 eV from the nominally type-II MQW samples with $(x,y)=(0.67,0.39)$ and (0.69,0.41). Neglecting small corrections (~15 meV) due to the electron and hole confinement energies, we estimate conduction band offsets of ~120–150 meV in these type-II structures. The general trends of the PL features as a function of excitation power have been reproduced from modeling of the quantum well electron and hole subband energies, including effects due to band bending at the heterointerfaces.

DOI: 10.1103/PhysRevB.74.235306 PACS number(s): 73.40.Kp, 73.21.Fg, 73.61.Ey

I. INTRODUCTION

Narrow band gap mixed alloys derived from the InAs/AlSb/GaSb family of semiconductors with lattice constants between 6.1 and 6.3 Å are of current interest for low-power, high-frequency device applications.[1] For example, these efforts have led to the development of InAs/AlSb high electron mobility transistors (HEMTs) with unity current gain frequency (f_T) of 90 GHz at a source-drain bias of only 100 mV (Ref. 2). In addition, *n-p-n* heterojunction bipolar transistors (HBTs) employing Be-doped $In_{0.27}Gas_{0.73}Sb$ for the base layer and quaternary layers of Te-doped $In_xAl_{1-x}As_ySb_{1-y}$ for the emitter and collector have been recently demonstrated.[3,4] A large appeal of this material system for the development of Sb-based HBTs is the flexibility to engineer the band gaps of the constituent layers and the conduction band offsets at the emitter/base and base/collector heterointerfaces. Based on an interpolation scheme[5,6] using the reported binary and ternary alloy band gaps and heterojunction offsets, the conduction band alignment at the ternary/quaternary interfaces is expected to be a sensitive function of the alloy composition while the valence band offset (~0.35 eV) is predicted to be much less sensitive. This leads to the possibility of either type-I or type-II band alignments at the emitter/base and base/collector interfaces. In particular, a small conduction band offset (Δ_{CB}) of ~100 meV has been predicted for the ($In_{0.27}Ga_{0.73}Sb/In_{0.69}Al_{0.31}As_{0.41}Sb_{0.59}$) base/emitter heterojunction employed in the initial design of 6.2 Å-based HBT structures.[7] While the InGaSb base layer is relatively easy to grow, the miscibility issues inherent to the mixed cation and anion alloys that comprise these quaternary emitter and collector layers pose a big challenge for nonequilibrium growth techniques such as molecular beam epitaxy (MBE). In addition, another critical issue is the choice of substrate (both GaAs and GaSb have been employed) for the epitaxial growth where lattice mismatch problems are expected for these 6.2 Å alloys.

In this work specially designed $In_{0.27}Ga_{0.73}Sb/In_xAl_{1-x}As_ySb_{1-y}$ multiple quantum well heterostructures were grown by MBE with the same alloy compositions as employed in the development of the 6.2-Å-based HBTs. The In/Al and As/Sb mole fractions were chosen based on predictions from theory for either type-I or type-II band alignments. In particular, for the type-I MQW structure both electrons and holes are expected to be located in the $In_{0.27}Ga_{0.73}Sb$ layers, while for the type-II heterostructures models predict localization of the electrons in the $In_xAl_{1-x}As_ySb_{1-y}$ quaternary layers and holes in the adjacent $In_{0.27}Ga_{0.73}Sb$ layers. Low-temperature photoluminescence (PL) studies as a function of excitation power were performed on these samples to confirm these band lineups and to provide the first measure of the conduction offsets in this material system. This approach is similar to that previously employed to determine the band offsets in type-I and type-II GaAsSb/InGaAs (Ref. 8) and GaAsSb/InP (Ref. 9) heterostructures, also of interest for electronic and optoelectronic device applications. Not including small corrections due to the electron and hole confinement energies, conduction band offsets of ~120 and 150 meV were found for the $In_{0.27}Ga_{0.73}Sb/In_xAl_{1-x}As_ySb_{1-y}$ heterointerfaces with $(x,y)=(0.67,0.39)$ and $(0.69,0.41)$, respectively.

II. EXPERIMENTAL DETAILS

The PL studies were performed on three 12-period (undoped) $In_{0.27}Ga_{0.73}Sb/In_xAl_{1-x}As_ySb_{1-y}$ MQW structures grown in a Riber solid-source MBE reactor with valved sources for cracked As_2 and Sb_2. The heterostructures were grown on semi-insulating GaAs substrates ($a_o=5.656$ Å) at 400 °C. For each sample an AlSb buffer layer of ~1 μm

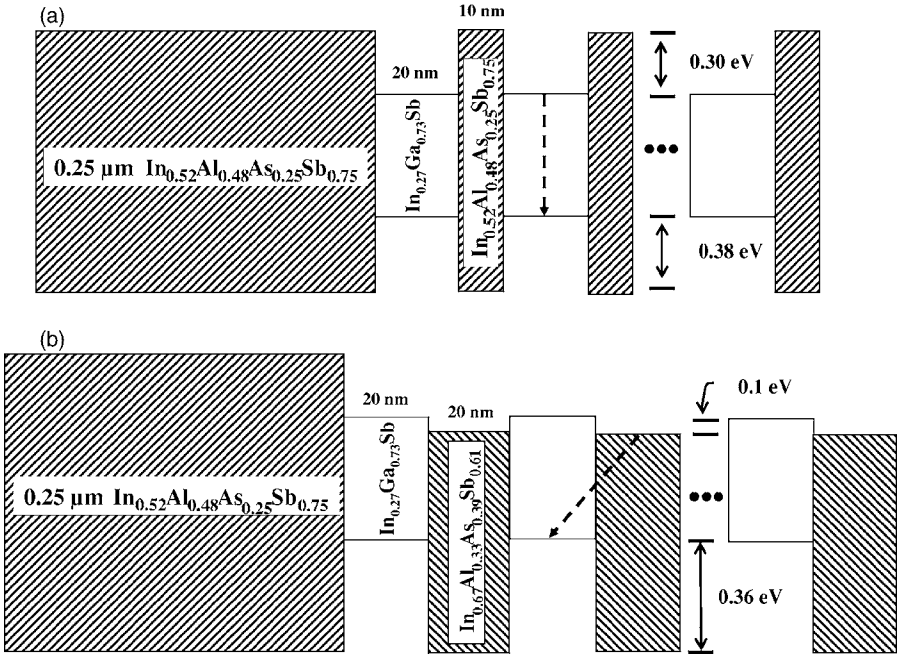

FIG. 1. Layer structure and energy band diagrams of $In_{0.27}Ga_{0.73}Sb/In_xAl_{1-x}As_ySb_{1-y}$ multiple quantum well samples investigated in this work. (a) "MQW A" with $(x,y)=(0.52,0.25)$ where a type-I band alignment is expected. (b) "MQW B" with $(x,y)=(0.67,0.39)$ where a type-II band lineup with electrons in the InAlAsSb layers and holes in the InGaSb layers is predicted ["MQW C" with $(x,y)=(0.69,0.41)$ is not shown]. Dashed arrows indicate lowest energy recombination process for each case.

was first deposited to accommodate part of the lattice mismatch. This was followed by a series of $In_xGa_{1-x}Sb$ layers, with x between 0.1 and 0.3 for grading of the lattice constant up to 6.2 Å. Prior to growth of the quantum wells, a 0.25-μm-thick (6.2 Å) $In_{0.52}Al_{0.48}As_{0.25}Sb_{0.75}$ quaternary layer was deposited for additional stress relief and to aid in confining the carriers to the quantum well region. The layer thicknesses, alloy compositions, and predicted band structure for $In_{0.27}Ga_{0.73}Sb/In_xAl_{1-x}As_ySb_{1-y}$ MQW samples A and B are shown schematically in Fig. 1. Sample A was designed with $(x,y)=(0.52,0.25)$ that is the composition used to form the emitter/base heterojunction (with type-I band alignment) of the 6.2 Å HBTs under development. Sample B was grown with $(x,y)=(0.67,0.39)$, which is expected to have a type-II band alignment relative to the $In_{0.27}Ga_{0.73}Sb$ layer. MQW sample C (not shown) is similar to sample B but with $(x,y)=(0.69,0.41)$, which is the composition used for the base/collector junction of the 6.2 Å HBT. The relatively thick dimensions of 200 Å for the ternary and quaternary layers of MQW samples B and C were chosen to minimize contributions to the PL transition energies from electron and hole confinement effects.

Several postgrowth structural characterization techniques were also performed on the three samples. These included atomic force microscopy to assess the surface morphologies, x-ray diffraction to provide the lattice constants and a measure of the crystalline quality, and secondary ion mass spectroscopy (SIMS)[10] to give the alloy compositions and layer thicknesses. In particular, the x-ray results revealed a single diffraction peak from the 100 and 200-Å-thick ternary and quaternary layers of the MQW samples corresponding to lattice constants between 6.208 and 6.217 Å (i.e., close to the design value of 6.2 Å). In addition, the SIMS was obtained under a high enough resolution to yield individual layer thicknesses of 190 Å for MQW samples B and C (i.e., within 5% of the intended values). The SIMS measurements were calibrated using InAlAs/InGaAs and InGaAsNSb reference standards with error limits of ±0.02 for the layer compositions employed in these samples.

The PL at 2 K was mainly excited with the 488-nm-line of an Ar^+ ion laser. Spectra were obtained with both unfocused (1.5 mm diam) and focused (~150 μm diam) light in order to vary the excitation power over several orders of magnitude. As confirmed by rough estimates of the absorption coefficients for the ternary and quaternary layers employed in these MQW samples, the 488-nm light was completely absorbed in the top few wells. In addition, due to the much longer penetration depth, PL from the underlying 0.25-μm-thick $In_{0.52}Al_{0.48}As_{0.25}Sb_{0.75}$ and 0.5-μm-thick $In_{0.27}Ga_{0.73}Sb$ buffer layers could be obtained with 1090-nm excitation from the Ar^+ laser. As discussed later, this was shown to be useful in order to possibly explain some of the additional lines observed from the MQW samples under 488-nm light excitation. The emission from 0.35–1.1 eV was analyzed by a $\frac{1}{4}$-m double-grating spectrometer using two sets of lined gratings and detected by LN_2-cooled InSb and Ge photodetectors. In order to avoid optical absorption due to water vapor, the optical path from the laser to the detectors was enclosed in plastic sheeting and flushed continuously with dry nitrogen gas. Finally, we note that all spectra were corrected for the system response by normalization to the throughput of a room-temperature black body source.

III. RESULTS AND DISCUSSION

Representative PL obtained at 2 K from $In_{0.27}Ga_{0.73}Sb/In_xAl_{1-x}As_ySb_{1-y}$ MQW samples A, B, and C with 488-nm excitation are shown in Fig. 2. Strong emission (labeled D) at 0.56 eV is observed from sample A with $(x,y)=(0.52,0.25)$. This energy is very close to the low-temperature band gap of bulk $In_{0.27}Ga_{0.73}Sb$, as reported in the literature from piezoreflectance measurements.[11] Thus, the strength of the PL and the energy are consistent with a

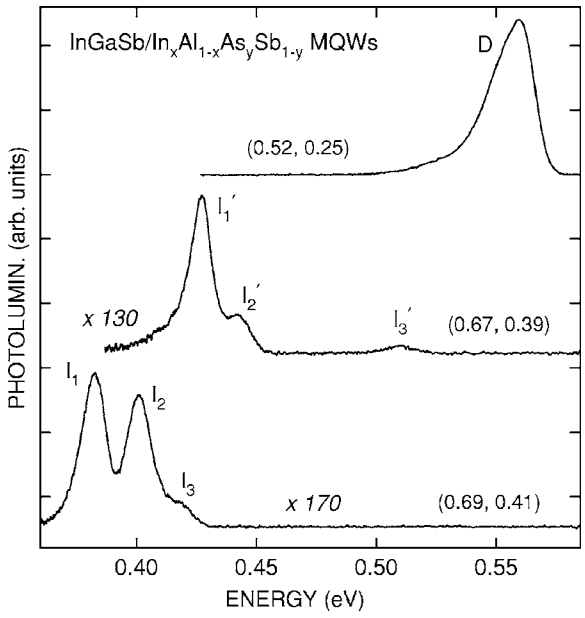

FIG. 2. Representative PL observed at 2 K from the three MQW samples with 488-nm excitation ($P_{\text{exc.}}=3$ mW). The labels for the various peaks refer to the nature of the transition: $D\equiv$ direct; I_x, $I_x' \equiv$ indirect.

type-I band alignment for this structure [as depicted in Fig. 1(a)] with spatially direct recombination of electrons and holes in the 200-Å-wide $In_{0.27}Ga_{0.73}Sb$ layers. Further support for this assignment comes from the weak dependence observed for the PL energy on excitation power density, as described in more detail below.

Significant differences are seen in the characteristics of the PL from MQW samples B and C with $(x,y)=(0.67,0.39)$ and (0.69,0.41), respectively, compared to that observed from sample A under the same excitation power conditions. First, the emission from both is approximately 150 times weaker. Second, multiple features are observed (labeled I_x' and I_x, where $x=1,2,\ldots$). Finally, the peak energies for most of these lines exhibit large shifts (>120 meV) to lower energy relative to the PL from sample A. We also note that low-temperature PL measurements were recently reported[12] for both undoped and Te-doped 1–2-μm-thick $In_xAl_{1-x}As_ySb_{1-y}$ epitaxial layers with the same In/Al and As/Sb composition ratios as employed in the quaternary layers for MQW samples B and C. Emission assigned to band-edge recombination near 0.75 eV was observed from these films, with *no* evidence for PL between 0.35 and 0.6 eV, as seen from samples B and C. Thus, the relative strengths *and* peak energies of the PL from MQW samples B and C are consistent with a type-II band alignment, as predicted for these structures [depicted in Fig. 1(b) for sample B] with all lines attributed to spatially indirect recombination involving electrons in the quaternary layers and holes in the adjacent ternary layers. Furthermore, a simple band structure calculation that includes band-bending effects, as discussed in more detail below, suggests that the multiplicity of lines reflects population of both the ground (E_0) and first excited (E_1) electron subbands in the $In_xAl_{1-x}As_ySb_{1-y}$ layers and the lowest energy hole subband (HH1) in the $In_{0.27}Ga_{0.73}Sb$ layers.

Further confirmation of the band alignments for these MQW samples and insights into the origin of the various emission bands were obtained from detailed power studies with 488-nm excitation. In particular, the single peak D from the MQW sample A exhibited a small shift to higher energy of ~15 meV as the power was varied from 1 to 2400 mW. This behavior is consistent with a type-I band alignment. In contrast to this sample, very rich spectra were found for MQW samples B and C as a function of excitation power with new peaks emerging at higher energy with increasing $P_{\text{exc.}}$. As shown in Fig. 3(a), only a single peak (I_x') at 0.420 eV was observed from sample B at the low excitation power of 0.3 mW. However, two additional lines (labeled I_2' and I_3') appeared at 0.440 and 0.510 eV with increasing excitation power, and these became the dominant features for $P_{\text{exc.}}$ higher than 500 mW. A multiplicity of PL lines was similarly observed from MQW sample C, as shown in Fig. 3(b). Two lines at 0.380 and 0.396 eV (labeled I_1 and I_2) were found under the lowest excitation power (0.1 mW) employed in this work. At higher powers a third feature (labeled I_3) emerged at ~0.42 eV. The intensity of this line increased significantly relative to that of I_1 and I_2 with increasing excitation power density. Finally, a fourth line (labeled I_4) near 0.5 eV appeared for excitation powers greater than 600 mW and, along with I_3, were the dominant emission bands observed under high excitation power conditions.

A plot of the PL energies for all three MQW samples as a function of excitation power density is shown in Fig. 4. An important characteristic expected for a type-II band alignment is large shifts to higher energy of the spatially indirect electron-hole recombination, especially at moderate to high photoinjected carrier densities. In short, the shift of the emission bands with increasing power density for type-II structures arises from the band bending that occurs at the heterointerfaces. This self-consistent Hartree potential results in shifts of the relative energies of the electron and hole states and leads to a shift of the PL bands to higher energy. This behavior has been reported, for example, from PL studies of other type-II semiconductor systems such as GaAs/AlAs short-period superlattices,[13] GaAsSb/InP heterostructures,[9] and self-assembled (In,Ga,Al)Sb quantum dots.[14] In further support of a type-II band structure, such shifts can be clearly seen in the present MQW structures for the I_2' and I_3' lines from sample B and for the I_3 and I_4 lines from sample C. However, the other peaks from these two samples (i.e., I_1' from sample B and I_1 and I_2 from sample C) only exhibit *weak* shifts to higher energy with increasing excitation power. These transitions are still attributed to type-II recombination processes whose possible origin will be discussed shortly.

Due to their pronounced shift with excitation power, as expected for such transitions with a type-II band alignment, we estimate the conduction band offsets for MQW samples B and C by subtraction of the I_2' and I_3 PL energies, respectively, obtained in the low excitation power limit from the $In_{0.27}Ga_{0.73}Sb$ direct band-gap energy of 0.56 eV. Not including a small correction of ~15 meV (in the low carrier density limit) due to the electron and hole confinement energies, this yields conduction band offsets of ~120 meV for sample B and ~150 meV for sample C. MQW sample C with

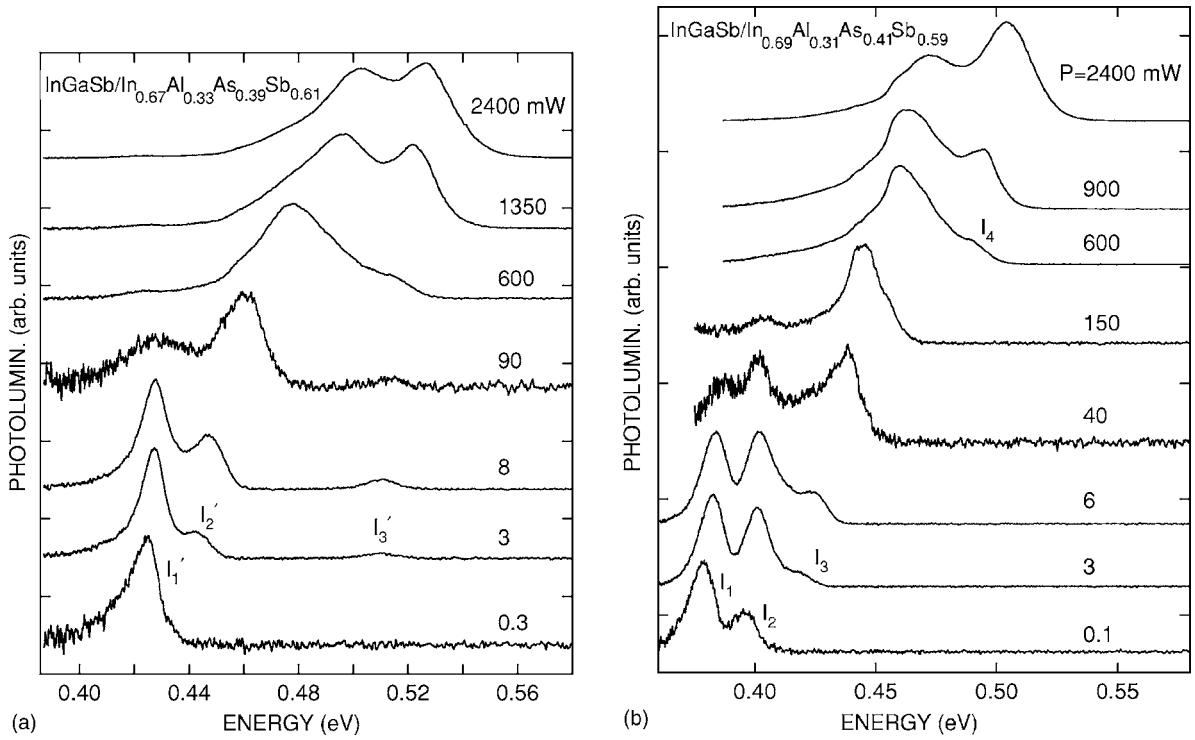

FIG. 3. PL spectra from $In_{0.27}Ga_{0.73}Sb/In_xAl_{1-x}As_ySb_{1-y}$ MQW samples B, $(x,y)=(0.67,0.39)$, and C, $(x,y)=(0.69,0.41)$ for several excitation powers.

slightly higher In and As compositions was specifically designed to demonstrate the tunability of the conduction band offset in this material system, of high importance for the development of the 6.2-Å HBTs. In particular, the models[6,7] predict a reduction in the quaternary band gap of ~40–50 meV with the small changes made in the In and As compositions between samples B and C. With the valence band offset only weakly dependent on the In/As and As/Sb ratios, one would expect this band-gap difference to be reflected nearly 100% in the corresponding increase of the conduction band offset at the ternary/quaternary heterointerfaces for sample C. The actual In composition increase between samples B and C revealed by SIMS was closer to 0.015 rather than the intended change of 0.02. Thus, the increase in Δ_{CBO} between MQW samples B and C of ~30 meV is in reasonable agreement with the change in quaternary band gap predicted from theory.

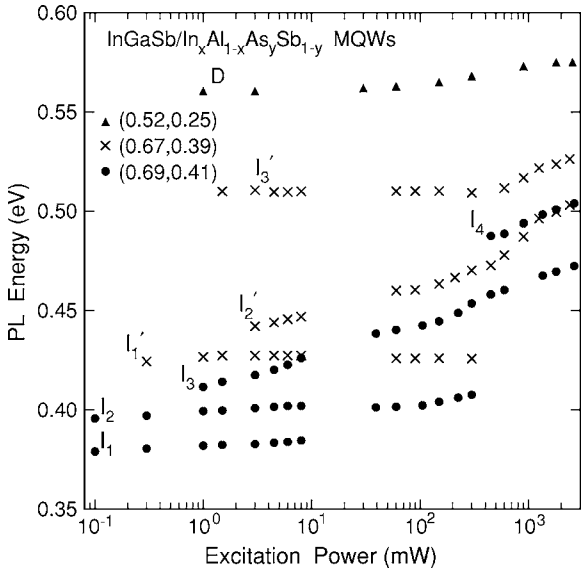

FIG. 4. The peak energies of the emission bands observed for the $In_{0.27}Ga_{0.73}Sb/In_xAl_{1-x}As_ySb_{1-y}$ MQW samples as a function of excitation power.

We note that it is also possible to estimate the valence band offsets (Δ_{VB}) in MQW samples B and C using the $In_{0.27}Ga_{0.73}Sb$ direct band-gap energy, the estimates given above for the conduction band offsets, and a knowledge of the 200-Å-thick quaternary alloy (direct) band-gap energies. However, band-edge recombination from these quaternary layers was not observed. Rough estimates of Δ_{VB} could still be made using the band-gap energies (~0.8 eV) obtained from PL studies of 1–2-μm-thick $In_xAl_{1-x}As_ySb_{1-y}$ layers with similar composition as employed in these two MQW samples. This procedure (again neglecting small corrections from the electron and hole confinement energies) yields Δ_{VB}'s of ~0.35 eV, in good agreement with that predicted from the interpolation schemes.

The origin of the various type-II transitions in samples B and C that exhibited large shifts under high excitation power conditions was aided by calculations[15] for the electron and hole subband energies in the quaternary and ternary layers, respectively, assuming a square well potential and using the conduction band offsets of 120 and 150 meV determined in this work. In addition, band-bending effects at the heterointerfaces were also included. A plot of the PL transition energies involving electrons from the ground (E_1) and first ex-

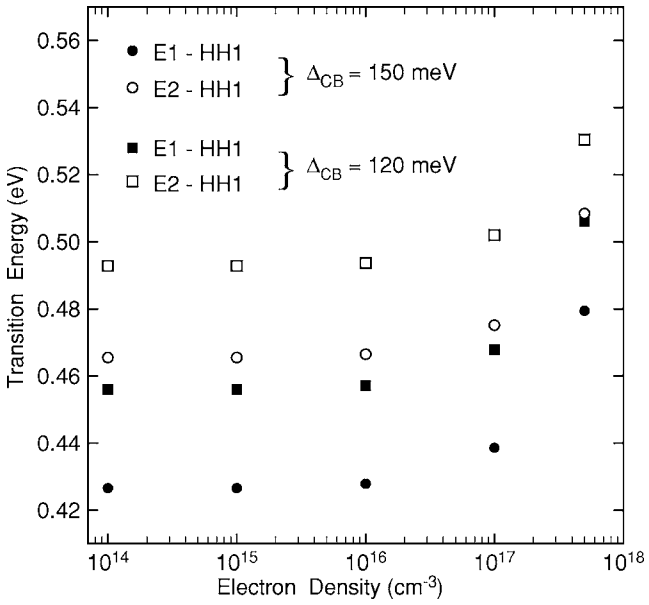

FIG. 5. Model of PL transition energies, including effects due to band banding, as a function of photoexcited carrier density for type-II recombination with electrons located in the $In_xAl_{1-x}As_ySb_{1-y}$ layers and holes located in the adjacent $In_{0.27}Ga_{0.73}Sb$ layers. Results are shown for conduction band offsets of 120 meV (squares) and 150 meV (circles).

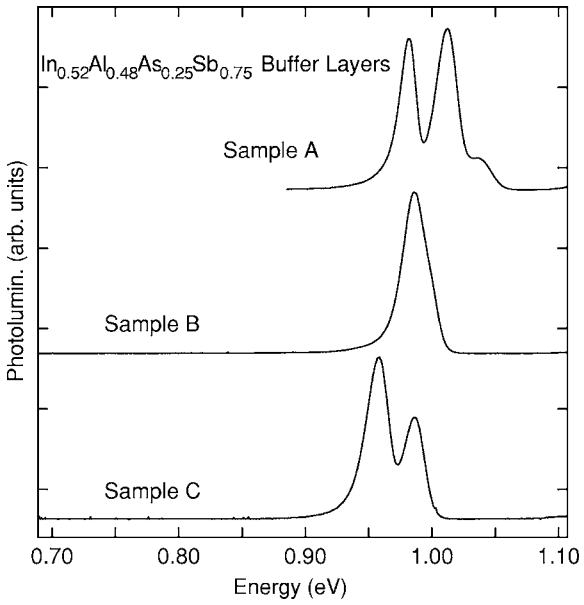

FIG. 6. Band-edge PL at 2 K from the 0.25-μm-thick (undoped) $In_{0.52}Al_{0.48}As_{0.25}Sb_{0.75}$ buffer layers of the three MQW samples obtained with 1090-nm excitation. The multiple features found for these layers near 1 eV are likely due to phase separation and possibly accounts for the additional low-energy indirect transitions observed from type-II MQW samples B and C.

cited (E_2) subbands in the quaternary layers and the heavy hole (HH1) subband in the ternary layer is shown in Fig. 5 as a function of photoinjected carrier density. The general trends observed for the I_2' and I_3' lines from sample B and for the I_3 and I_4 lines from sample C are reproduced in this model, including the weak shift of the lines under low photocreated carrier densities *and* the large shift with high photoexcitation. We note that the model predicts an E_2–E_1 splitting of $\sim$ 25–30 meV in the high excitation power regime for these two samples. This is approximately the energy difference observed between I_3' and I_2' in sample B and the I_4 and I_3 lines in sample C with excitation powers close to 1000 W and above. Thus, we assign features I_2' and I_3' from MQW sample B to radiative recombination involving electrons from the ground (E1) and first excited (E2) electron subbands, respectively, in the quaternary layers and holes from the ground heavy hole subband (HH1) in the adjacent ternary layers. Similarly, for MQW sample C, I_3 and I_4 are ascribed to PL transitions involving electrons from the E1 and E2 subbands, respectively, in the $In_{0.69}Al_{0.31}As_{0.41}Sb_{0.59}$ layers and holes from the HH1 subband in the $In_{0.27}Ga_{0.73}Sb$ layers.

As noted earlier, the other low-energy PL transitions found between 0.37 and 0.42 eV from MQW samples B (i.e., I_1') and C (i.e., I_1 and I_2) that exhibit small shifts but strong saturation behaviors with increasing excitation power are still attributed to type-II recombination. Two possible mechanisms for the origin of these lines with such characteristics have been considered. The first is that these are impurity-related features. However, separate PL studies of 1–2-μm-thick undoped and doped (Te and Be) $In_xAl_{1-x}As_ySb_{1-y}$ and $In_{0.27}Ga_{0.73}Sb$ films did not reveal evidence for below-band-gap emission between 0.35 and 0.44 eV. A second mechanism to account for these lines is the possibility of phase separation within the 200-Å-thick $In_xAl_{1-x}As_ySb_{1-y}$ layers of the MQWs that would give rise to two or more distinct alloy compositions. Based on the small energy separation ($\sim$10–20 meV) found between the I_1'–I_2' and I_1–I_3 PL lines and the low-temperature band-gap energies reported recently for $In_xAl_{1-x}As_ySb_{1-y}$ epitaxial layers[12] with similar compositions as employed in these MQW samples, the corresponding compositional change for these phase-separated regions would be quite small (i.e., less than a few percent). Thus, in this model, the low-energy (indirect) transitions in MQW samples B and C would arise from electrons located in regions of the $In_xAl_{1-x}As_ySb_{1-y}$ layers with the highest In/Al and/or As/Sb ratios. We note that small compositional changes in the quaternary layers of MQW sample A would have no effect on the PL energy given that the radiative recombination occurs entirely within the InGaSb layers for that structure. Evidence for the possible existence of compositional fluctuations within the 200-Å-thick quaternary layers of the MQWs was found from the band-edge PL of the underlying 0.25-μm-thick $In_{0.52}Al_{0.48}As_{0.25}Sb_{0.75}$ buffer layers. Representative spectra obtained from these layers for all three MQW samples with 1090-nm excitation are shown in Fig. 6. Most notably, the observation of multiple PL lines near the expected band gap of 1.0 eV from the $In_{0.52}Al_{0.48}As_{0.25}Sb_{0.75}$ buffer layers of MQW samples A and C strongly suggests the possibility of the existence of similar growth-induced phase separation in the quaternary layers of the MQWs. This would not be surprising given the miscibility problems expected for this material system.

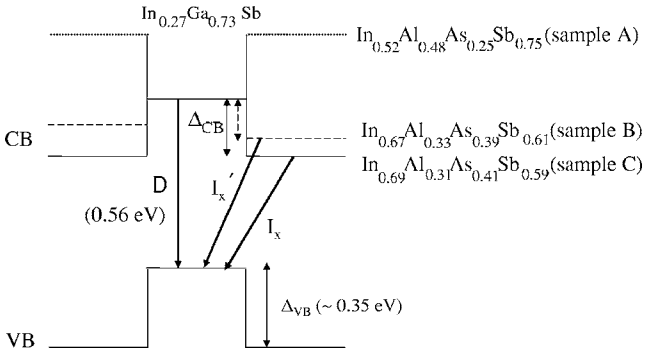

FIG. 7. Schematic band-edge profiles based on PL results for the three $In_{0.27}Ga_{0.73}Sb/In_xAl_{1-x}As_ySb_{1-y}$ MQW samples.

IV. SUMMARY

Low-temperature PL as a function of excitation power has been performed on a set of $In_{0.27}Ga_{0.73}Sb/In_xAl_{1-x}As_ySb_{1-y}$ MQW heterostructures grown by MBE to provide a measure of the conduction and valence band offsets. A schematic representation that summarizes the various PL lines and the conduction and valence band-edge profiles for all three samples is shown in Fig. 7. The strong emission (peak D) at ~0.56 eV from sample A with $(x,y)=(0.52,0.48)$ is consistent with a type-I band alignment where the lowest energy electron and hole states are located in the $In_{0.27}Ga_{0.73}Sb$ quantum well layers. In contrast, the weaker PL lines (labeled I'_x and I_x, where $x=1,2,3,\ldots$) observed at lower energies from MQW samples B and C with $(x,y)=(0.67,0.39)$ and $(0.69,0.41)$, respectively, are attributed to spatially indirect recombination involving electrons from the quaternary layers and holes from the adjacent ternary layers. This type-II band alignment with conduction band offsets of 100–150 meV is consistent with that predicted by theory. Most notably, these results demonstrate the tunability of the conduction band offset with small changes in the In/Al and As/Sb composition ratios and, thus, the design flexibility available for the ongoing development of 6.2-Å-based heterojunction bipolar transistors.

ACKNOWLEDGMENT

This work was supported by the U.S. Office of Naval Research.

[1] For a recent review, see B. R. Bennett, R. Magno, J. B. Boos, W. Kruppa, and M. G. Ancona, Solid-State Electron. **49**, 1875 (2005).
[2] J. B. Boos, B. R. Bennett, W. Kruppa, D. Park, J. Mittereder, R. Bass, and M. E. Twigg, J. Vac. Sci. Technol. B **17**, 1022 (1999).
[3] R. Magno, J. B. Boos, P. M. Campbell, B. R. Bennett, E. R. Glaser, B. P. Tinkham, M. G. Ancona, K. Hobart, D. Park, N. A. Papanicolaou, and B. V. Shanabrook, Electron. Lett. **41**, 370 (2005).
[4] R. Magno, E. R. Glaser, B. P. Tinkham, J. G. Champlain, J. B. Boos, M. G. Ancona, and P. M. Campbell, J. Vac. Sci. Technol. B **24**, 1622 (2006).
[5] T. H. Glisson, J. R. Hauser, M. A. Littlejohn, and C. K. Williams, J. Electron. Mater. **7**, 1 (1978).
[6] I. Vurgaftman, J. R. Meyer, and L. R. Ram-Mohan, J. Appl. Phys. **89**, 5815 (2001).
[7] R. Magno, B. R. Bennett, K. Ikossi, M. G. Ancona, E. R. Glaser, N. Papanicolaou, J. B. Boos, B. V. Shanabrook, and A. Gutierrez, in *Proceedings of the IEEE Lester Eastman Conference on High Performance Devices 2002*, edited by R. E. Leoni III (IEEE, Piscataway, NJ, 2003), pp. 288–296.
[8] J. Hu, X. G. Xu, J. A. H. Stotz, S. P. Watkins, A. E. Curzon, M. L. Thewalt, N. Matine, and C. R. Bolognesi, Appl. Phys. Lett. **73**, 2799 (1998).
[9] M. Peter, N. Herres, F. Fuchs, K. Winkler, K.-H. Bachem, and J. Wagner, Appl. Phys. Lett. **74**, 410 (1999).
[10] SIMS measurements were performed at Charles Evans and Associates, West.
[11] D. Auvergne, J. Camasse, H. Mathieu, and A. Joullie, J. Phys. Chem. Solids **35**, 133 (1974).
[12] E. R. Glaser, R. Magno, B. V. Shanabrook, and J. G. Tischler, J. Vac. Sci. Technol. B **24**, 1604 (2006).
[13] See, for example, R. Teisser, R. Planel, and F. Mollot, Superlattices Microstruct. **12**, 539 (1992).
[14] E. R. Glaser, B. R. Bennett, B. V. Shanabrook, and R. Magno, Appl. Phys. Lett. **68**, 3614 (1996).
[15] 1D Poisson FreeWare Program, http://www.nd.edu/~gsnider/.